

Supporting Information: Exploiting Shape-Selected Iron Oxide Nanoparticles for the Destruction of Robust Bacterial Biofilms – Active Transport of Biocides via Surface Charge and Magnetic Field Control

Rachel Nickel, Mohammad Kazemian, Yaroslav Wroczynskyj, Song Liu, and Johan van Lierop

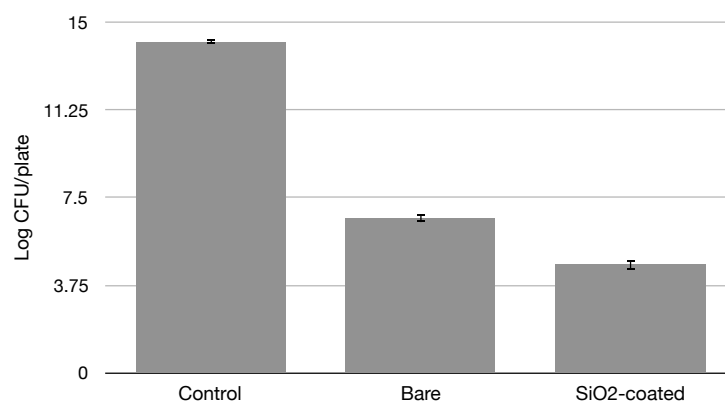


Figure S1: Biofilm test results of 30 mg ml⁻¹ bare and SiO₂-coated iron oxide nanoparticles in a rotating magnetic field. During treatment with rotating magnetic field, reduced mobility was observed for the bare nanoparticles indicating that aggregation impairs the nanoparticles' ability to inflict physical damage.

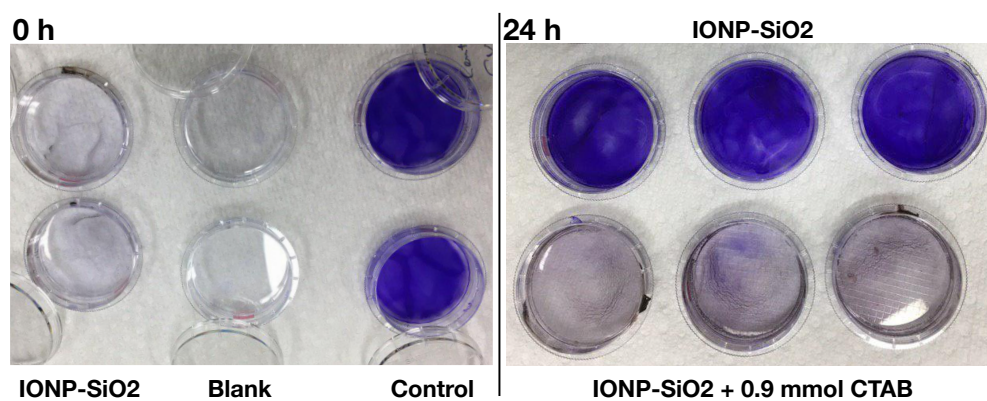


Figure S2: (left) Crystal violet (CV) stained MRSA biofilm after treatment with 30 mg ml^{-1} SiO_2 -coated iron oxide spheres (IONP- SiO_2), blank polystyrene dish (negative control), and untreated MRSA biofilm (positive control) immediately after treatment. (right) CV stained MRSA biofilm incubated 24 h after treatment of 30 mg ml^{-1} SiO_2 -coated iron oxide spheres and 30 mg ml^{-1} SiO_2 -coated iron oxide spheres + 0.9 mmol CTAB. Control films at 0 h are nearly indistinguishable from IONP- SiO_2 treated films at 24 h.

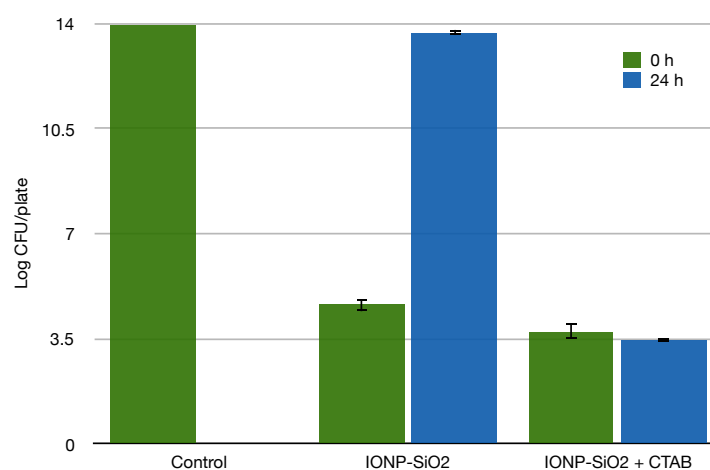


Figure S3: Biofilm test results using iron oxide nanoparticles (IONP- SiO_2) with and without CTAB in a rotating magnetic field immediately after treatment (0 h) and after 24 h of incubation. Films treated with IONP- SiO_2 have almost fully recovered, while the addition of CTAB inhibits growth.

Table S1: Lognormal fit parameters of size distributions for spheres, cubes and tetrapods. Size denotes diameter for spheres, and side length for cubes and tetrapods. The lognormal distribution was defined by $y = y_0 + A \exp\left(-\left[\frac{\ln(x/x_0)}{W}\right]^2\right)$, where y_0 and A are normalization terms, x_0 is the mode, and W describes the width of the distribution.

Shape	y_0	A	x_0 (nm)	W
Sphere	7 ± 4	91 ± 8	22.0 ± 0.2	0.14 ± 0.01
Cube	0 ± 1	89 ± 2	7.73 ± 0.05	0.35 ± 0.01
Tetrapod	0 ± 4	75 ± 5	13.1 ± 0.2	0.32 ± 0.03

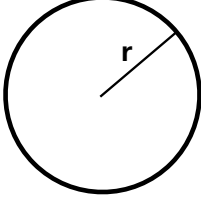
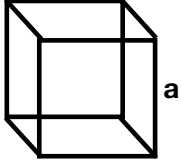
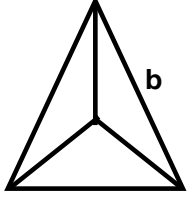
		
$V = \frac{4\pi r^3}{3}$	$V = a^3$	$V = \frac{b^3}{6\sqrt{2}}$
$SA = 4\pi r^2$	$SA = 6a^2$	$SA = \sqrt{3}b^2$
$L = 0$	$L = 8a$	$L = 6b$

Figure S4: Schematic of model shapes and corresponding equations to calculate volumes, surface areas and edge lengths.

Table S2: Calculated parameters for model nanoparticles.

Shape	Average Radius/Side Length (nm)	Volume (nm ³)	Surface Area (nm ²)	Edge Length (nm)
Sphere	11.0 ± 0.1	5600 ± 200	1520 ± 20	—
Cube	7.73 ± 0.05	461 ± 9	358 ± 4	61.8 ± 0.4
Tetrapod	13.1 ± 0.2	270 ± 10	298 ± 7	79 ± 1

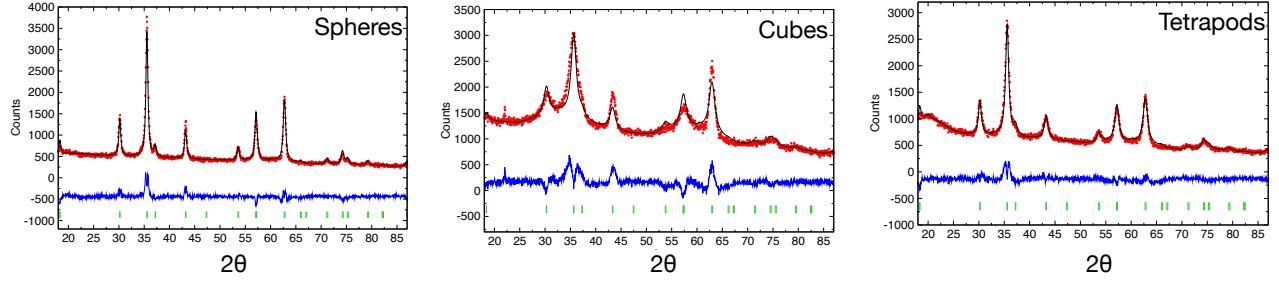


Figure S5: X-ray diffraction patterns of spheres, cubes and tetrapods. Red dots are data and black line indicates fit. The green Bragg markers index the $Fd\bar{3}m$ structure while the blue line is the residuals of the refinement. Scherrer analysis incorporated into the refinements identified that the average crystallite sizes of the spheres, cubes and tetrapods were 13.1 ± 0.2 nm, 4.77 ± 0.09 nm, and 12.3 ± 0.8 nm, respectively. Pattern mismatch with the cubes is attributed to strain effects.¹

¹ Zak, A. K.; Majid, W. A.; Abrishami, M. E.; Yousefi, R. X-ray analysis of ZnO nanoparticles by Williamson–Hall and size–strain plot methods. *Solid State Sciences* **2011**, *13*, 251–256

Factors affecting M_S :

The magnetic saturation values for the spheres, cubes and tetrapods are 37.9 ± 0.2 Am² kg^{−1}, 29.7 ± 0.7 Am² kg^{−1} and 18.2 ± 0.2 Am² kg^{−1}, respectively. Using the mean diameter and side lengths of the nanoparticles, only $\sim 22\%$ of the spheres' Fe ions (Fe²⁺ and Fe³⁺ via superexchange are responsible for the ferrimagnetism of the nanoparticles) are on or near the surface (within a unit cell), compared to $\sim 65\%$ of the cubes' Fe ions, and $\sim 94\%$ of the tetrapods Fe ions being on the surface, respectively (see Tables S3 and S4 for calculation details). The surface Fe ions suffer broken coordination environments and magnetic frustration, and this disorder decreases the number of ions that can contribute to the overall magnetic response. Thus the reduced M_S of the cubes and tetrapods is due to surface spin disorder, related to finite size effects from the more complex morphology and edge discontinuities.

Table S3: Calculated percent surface Fe ions for model nanoparticles. Surface volume is the product of the calculated surface area and the unit cell length of Fe₃O₄ (0.083919 nm). Since the number of Fe ions in a unit cell is constant (24 Fe ions/unit cell), the ratio of surface volume to total volume gives the percentage of Fe ions found within one unit cell of the surface.

Shape	Total Volume (nm ³)	Surface Volume (nm ³)	% Surface Fe Ions
Sphere	5600 ± 200	1280 ± 10	22.9 ± 0.7
Cube	461 ± 9	301 ± 4	65 ± 1
Tetrapod	270 ± 10	250 ± 6	94 ± 5

Table S4: Normalized calculated ratios for model nanoparticles.

Shape	Surface Area/Volume (nm ^{−1})	Edge Length/Volume (nm ^{−2})	Edge Length/Surface Area (nm ^{−1})
Sphere	0.243 ± 0.007	0	0
Cube	0.69 ± 0.02	0.453 ± 0.009	0.653 ± 0.009
Tetrapod	1.00 ± 0.05	1.00 ± 0.05	1.00 ± 0.03

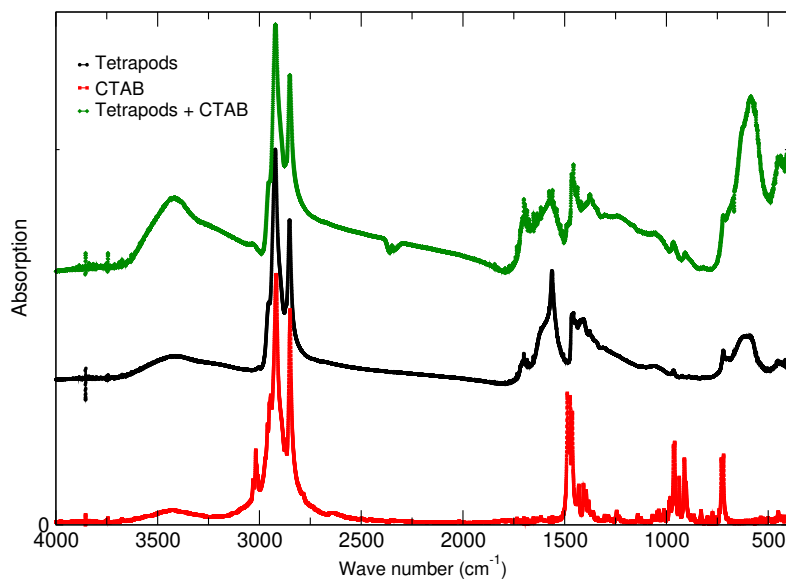


Figure S6: Full FTIR spectra of tetrapods before and after CTAB loading, as well as pure CTAB.

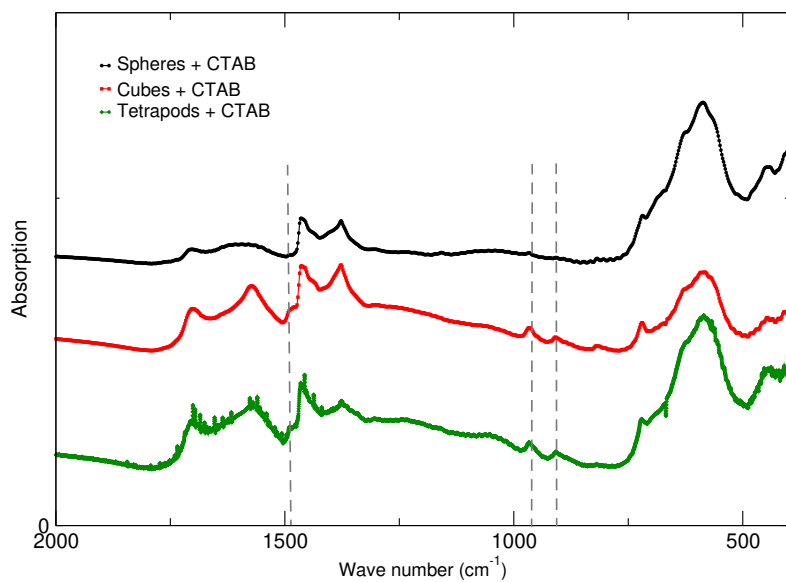


Figure S7: Low frequency FTIR spectra of spheres, cubes and tetrapods after CTAB loading. Characteristic CTAB bands at 908, 968 and 1489 cm^{-1} are marked.